Erratum: Varied domain structures in 0.7Pb($Mg_{1/3}Nb_{2/3}$)O_3-0.3$PbTiO_3$ single crystals

Dawei Zhang[1,2,#], Lei Wang[1,#], Linglong Li[3], Pankaj Sharma[4,5], Jan Seidel[1,2]

[1]School of Materials Science and Engineering, UNSW Sydney, Sydney, NSW 2052, Australia.

[2]ARC Centre of Excellence in Future Low-Energy Electronics Technologies, UNSW Sydney, Sydney, NSW 2052, Australia.

[3]Key Laboratory of Quantum Materials and Devices of Ministry of Education, School of Physics, Southeast University, Nanjing 211189, Jiangsu, China.

[4]College of Science and Engineering, Flinders University, Bedford Park, Adelaide, SA 5042, Australia.

[5]Flinders Institute for Nanoscale Science and Technology, Flinders University, Adelaide, SA 5042, Australia.

[#]Authors contributed equally.

Correspondence to: Prof. Jan Seidel, School of Materials Science and Engineering, UNSW Sydney, Sydney, NSW 2052, Australia. E-mail: jan.seidel@unsw.edu.au

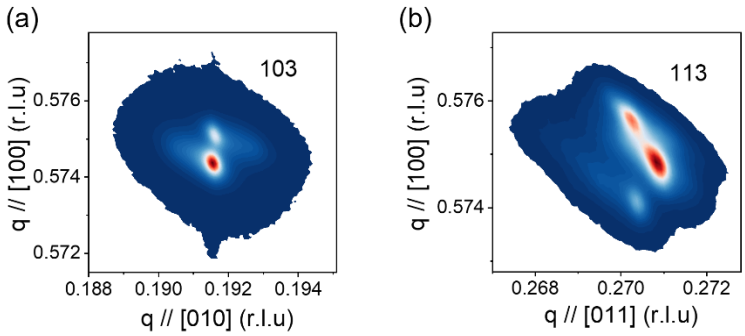

Figure S1. (a) and (b) RSM maps around 103 and 113 reflections of the single crystal, respectively.

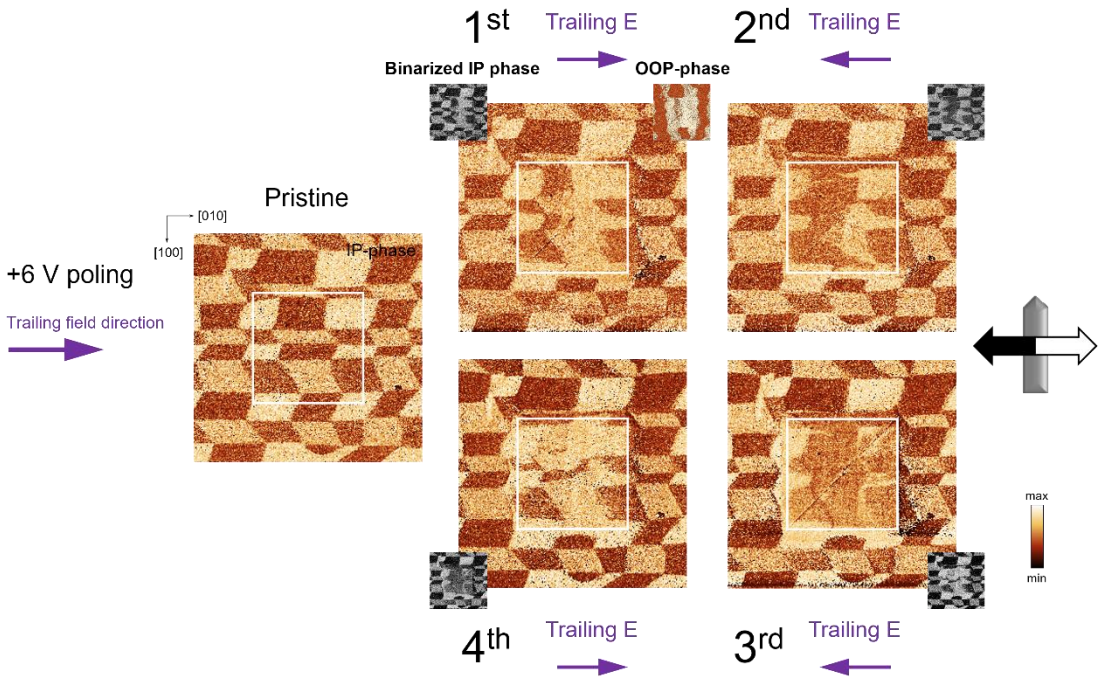

Figure S3. The trailing field experiment to determine the directions of the IP phase contrast. All the phase images shown here are IP phase signals unless otherwise denoted. All the measurements shown here were performed at off-resonance frequency. A tip bias of +6 V was used to pole the sample, and the trailing field direction was co-determined by the slow scan axis of the tip and the polarity of the tip bias, as denoted by the purple arrow. The trailing field experiments were performed four times in the denoted sequence. The original data was shown in the insets beside the binarized data. By comparing the directions of the trailing field and the resultant binarized contrast, the directions of the IP phase contrast can be determined.

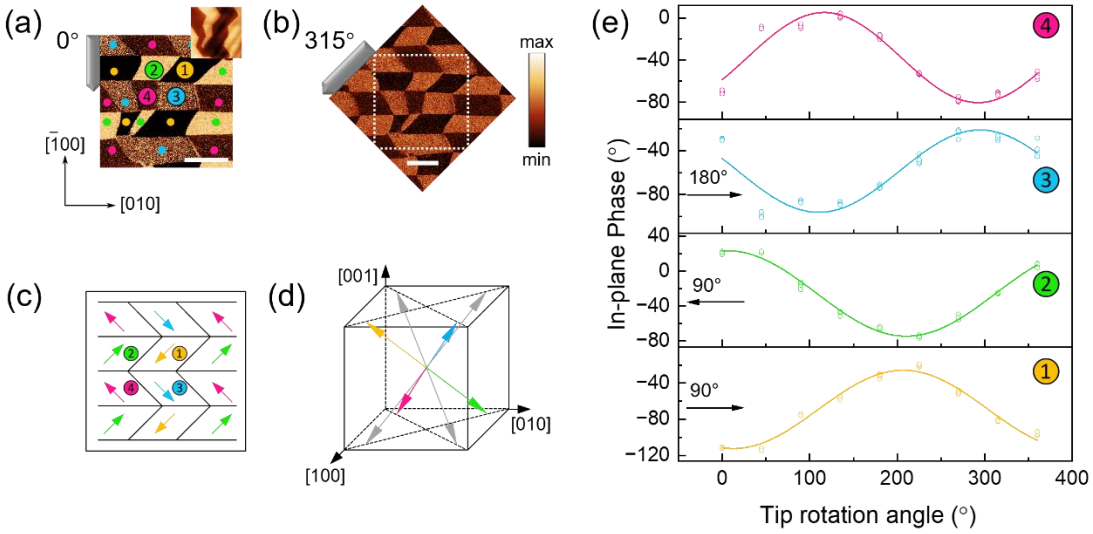

Figure S5. The domain and crystal structure of the PMN-PT single crystal. (a)-(b) Representative angle-resolved IP phase images of 0° and 315°. The white dashed boxes delineate the quasi-identical scanned area at 0°. The topography is also shown as an inset for the 0° IP phase. Cantilevers show sample rotation angles with respect to the [00$\bar{1}$] direction. All the domains can be classified into four categories depending on their polarization variants (colored dots). Both scale bars are 2 μm. (c) IP polarization directions for the four types of domains. (d) Three-dimensional model for polarization vectors in the PMN-PT single crystal. (e) Angle-dependent in-plane signals of four different domains are fitted to a trigonometric curve.

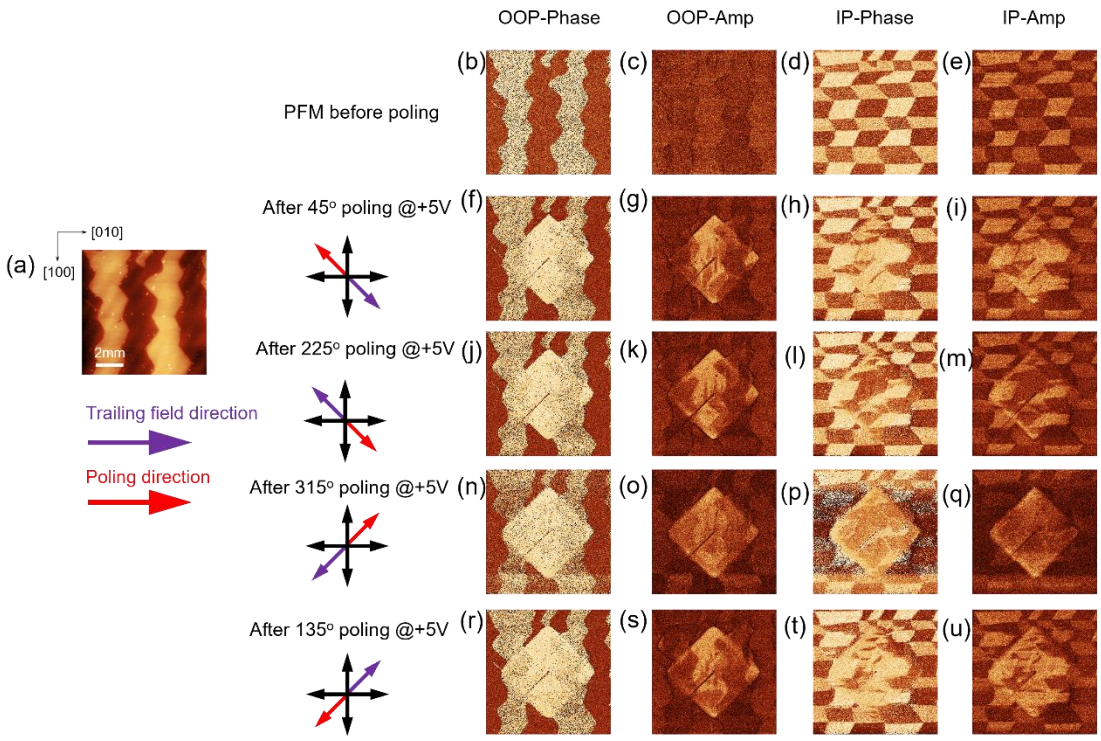

Figure S6. Trailing field experiments at +5 V with different angles. (a) The topography of the scanned area. (b)-(e) PFM images for the pristine state before DC poling. (f)-(i) PFM images after +5V poling with a 45° rotation angle. (j)-(m) PFM images after +5V poling with a 225° rotation angle. (n)-(q) PFM images after +5V poling with a 315° rotation angle. (r)-(u) PFM images after +5V poling with a 135° rotation angle. The purple and red arrows indicate the directions of the trailing field and poling field, respectively.

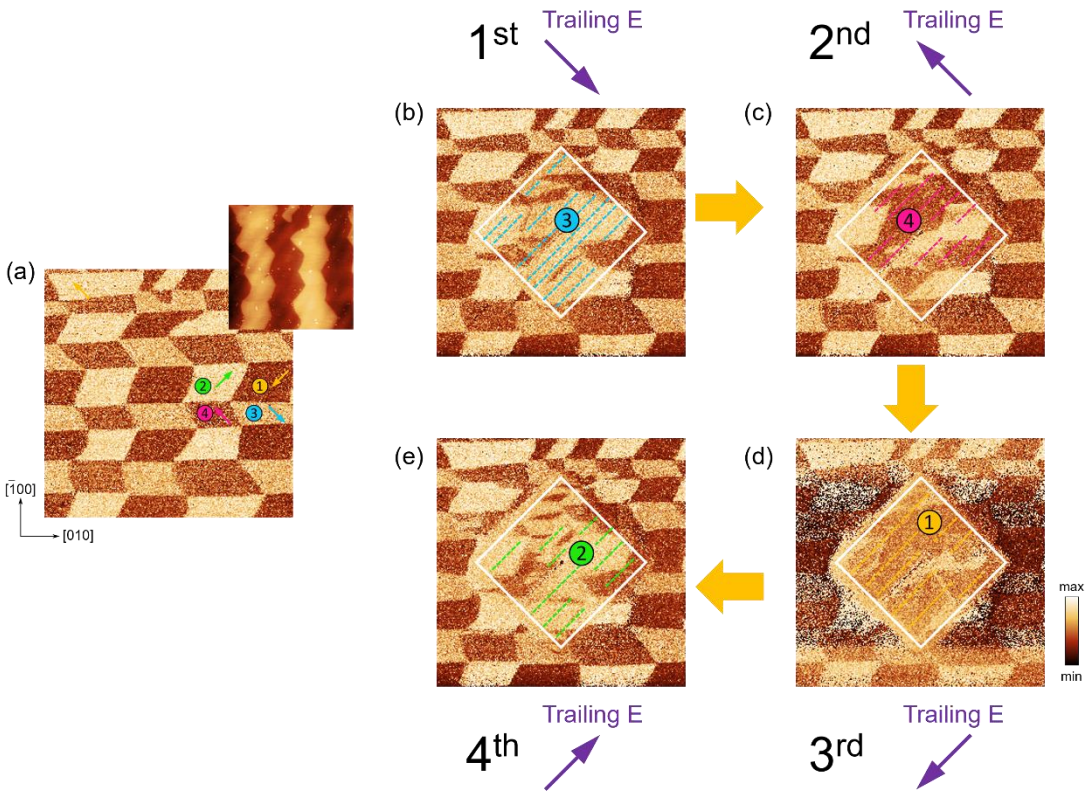

Figure S7. The analysis of the trailing field experiments. (a) The IP-phase image of the pristine state with the direction of four polarization variants is indicated by the color arrows. (b)-(e) Trailing field experiments at +5 V with different rotation angles in sequence. The purple arrows in (b)-(e) show the directions of the trailing fields. The respective colors and dashed lines inside the poling area (delineated by the white dashed boxes) denote the IP polarization favored by the direction of the trailing fields.